Electron holography of core-shell Co/CoO spherical nanocrystals

Youhui Gao[a)]
Department of Physics, Beijing Normal University, Beijing 100875, People's Republic of China

Daisuke Shindo
Institute of Multidisciplinary Research for Advanced Materials, Tohoku University, Sendai 980-8577, Japan

Yuping Bao
Center for Integrated Nanotechnologies-Biomaterials, MPA Division, MS K771, Los Alamos National Laboratory, Los Alamos, New Mexico 87545

Kannan Krishnan
Department of Materials Science and Engineering, Box 352120, University of Washington, Seattle, Washington 98195

(Received 27 March 2007; accepted 20 April 2007; published online 5 June 2007)

Phase profiles of core-shell Co/CoO nanocrystals are imaged using off-axis electron holography. Contributions of mean inner potential and magnetic induction to the phase shift are extracted, respectively, to quantitatively characterize the nanocrystal geometry and magnetic spin arrangement in a self-assembled nanocrystal chain. It is also found that the spin of 11 nm diameter Co core encapsulated with 5-nm-thick CoO shell remains stable even at an elevated temperature of 200 °C, indicating that the magnetically thermal stability of cobalt nanocrystals is remarkably improved due to the exchange coupling between the ferromagnetic core and antiferromagnetic shell. © *2007 American Institute of Physics*. [DOI: 10.1063/1.2747052]

Core-shell magnetic nanocrystal (CsMN) is a heterostructure in which a magnetic core is encapsulated with a shell of different composition.[1–4] The shell selected from many alternatives, such as ferro/ferrimagnetic,[5,6] antiferromagnetic,[7] or nonmagnetic materials,[8,9] can readily tailor the surface properties of the nanocrystal and improve the overall physical and chemical properties of the core-shell structure. It has recently been shown that the thermal stability of a ferromagnetic (FM) core can be improved by an antiferromagnetic (AFM) coating layer due to the fact that the exchange coupling between them results in a large effective anisotropy energy KV,[7] where K and V are the effective anisotropic constant and the volume of the core, respectively. With an optimum interface between the FM core and the AFM shell, the exchange coupling could lead to magnetically stable nanocrystals only a few nanometers in diameter. Thus, recording byte size in the media of such nanocrystals could be decreased by several orders, and the storage goal of 1 Tbyte/in.^{2} would be easily achieved.[10] The CsMNs are promising building blocks for the bottom-up synthesis of nanostructured materials and devices with novel functions for ultrahigh-density magnetic storage, spintronics, and biomedical applications. Such application requires not only advances in the synthesis of CsMNs but also the development of sophisticated methods of characterizing the magnetic structure, especially to understand the self-assembling behavior and the bulk magnetic properties of CsMN arrays. In this letter, we use off-axis electron holography in the transmission electron microscope (TEM), a technique that provides high-resolution information about materials and analyze local magnetic and electric nanofields, to record phase shift of a high-energy electron wave that has passed through Co/CoO core-shell nanocrystals. The core-shell nanocrystal geometry and spin arrangement in a self-assembled nanocrystal chain are *quantitatively* characterized with the phase shift profiles.

CsMN of Co/CoO was synthesized utilizing a procedure similar to the one reported elsewhere.[11,12] 1.58 mmol (0.54 g) of cobalt carbonyl was dissolved in 3 ml of 1,2-diclrorobenzene (DCB), forming a precursor stock solution. The stock solution was then injected into preheated DCB (180 °C) solution containing a mixture of 0.26 mmol (0.1 g) of tri-*n*-octylphosphine oxide (TOPO) and refluxed for 1 h. The whole procedure was carried out in an inert atmosphere. 20 nm nanocrystals with a narrow size distribution (standard deviation $<5\%$) were obtained by controlling the reaction time. A CoO layer was subsequently formed over time once the nanoparticle solution was exposed to air, due to the fact that the bulky tails of the TOPO coatings allowed easy penetration of oxygen.[12] The partially oxidized cobalt nanoparticle was finally deposited onto amorphous carbon-coated copper TEM grids by a gradient evaporation process.[13,14]

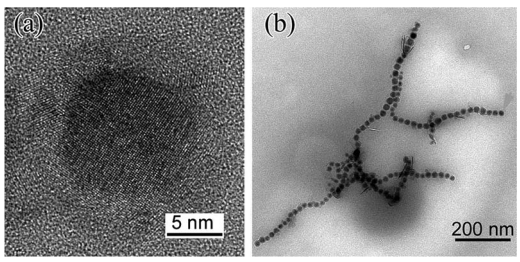

FIG. 1. High-resolution TEM image (a) indicates the core-shell Co/CoO microstructure, in which the nanocrystal observed is arrowed in (b). TEM image (b) shows Co/CoO nanocrystal chains self-assembled by magnetic dipolar interaction. It is found that the core of ε-Co is about 10 nm in diameter and the oxygen-rich shell is about 5 nm in thickness.

[a)]Electronic mail: ygao@bnu.edu.cn

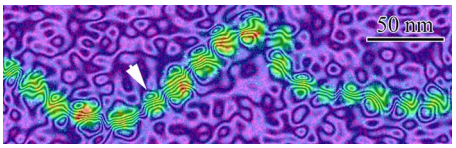

FIG. 2. (Color online) Reconstructed phase image of the electron holography carried out at room temperature at an accelerating voltage of 200 kV with a JEM 3000F field-emission-gun TEM, which is equipped with a special pole piece to shield the sample from the field of the objective lens. A positive voltage of 40 V is applied to an electrostatic biprism wire. The arrowed nanocrystal is analyzed in Fig. 3.

High-resolution TEM (HRTEM) clearly indicates the core-shell structure of the Co/CoO particles [see Fig. 1(a)]. It is found that the spherical core is perfectly crystallized and indexed as ε-Co, a metastable cubic structure isomorphous with β-Mn.[15] An elemental map obtained by energy-filtered TEM analysis reveals that the oxygen-rich shell is about 5 nm in thickness. The above dispersion condition produces self-assembled nanocrystal chains with an average interparticle distance of 4 nm [Fig. 1(b)], which results from the balance of competing weak interactions including the interparticle magnetostatic dipolar interactions, the van der Waals attraction, and the steric repulsive force of the surfactant. The formation of the chains also indicates that the magnetic spins of these core-shell nanoparticles are blocked in the direction of the effective easy axis, even though the cobalt core is less than 12 nm, and just below the characteristic size for superparamagnetic behavior, according to the HRTEM image. The direct observation of the distribution of spins in a Co/CoO nanoparticle chains by off-axis electron holography is reported in this letter. This technique has been used to visualize magnetic flux with nanometer spatial resolution.[16–18]

The electron holography was carried out at an accelerating voltage of 200 kV with a JEM 3000F field-emission-gun TEM, which was equipped with a special pole piece to shield the sample from the magnetic field of the objective lens. Such pole piece reduced the lens field to about 0.6 mT although the objective lens was turned on to improve the resolution (~2 nm). Thus, the effect of the background on the accuracy of observation data can be neglected in this experiment. A positive voltage of 40 V was applied to an electrostatic biprism wire in order to overlap the object electron wave with the reference wave. The phase shift arises from both the mean inner potential (ϕ_{MIP}) and from the magnetic induction (ϕ_{mag}) of Co/CoO nanocrystals, and is given by the following expression.[17]

$$\phi_{\mathrm{total}}(x,y) = \frac{2\pi}{\lambda U(1+\sqrt{1-(v/c)^2})}\int V(x,y,z)dz + \frac{e}{\hbar}\int\int B_n ds, \quad (1)$$

where B_n is in-plane component of the magnetic induction, z is the incident electron beam direction, U is the TEM accelerating voltage, λ is the wavelength, and v and c are electron and light velocities. The first term ϕ_{MIP} is proportional to the specimen thickness, portraying the nanocrystal geometry in the electron beam direction. The second term ϕ_{mag} is proportional to the in-plane component of the magnetic induction B_n integrated in the electron beam direction. Its reconstructed phase image provides a quantitative measure of the strength and the direction of the local magnetic flux density. In the present study ϕ_{MIP} and ϕ_{mag} are, respectively, extracted from the total phase shift ϕ_{total} in order to quantatively analyze the Co/CoO nanocrystals.

Reconstructed phase image of ϕ_{mag} is shown in Fig. 2, which was obtained only from the magnetic contribution to the phase shift when the nanocrystals were observed at the magnetic remanent state. Continuous contours running through the whole particle chain are observed, suggesting that the nanocrystal spins are aligned head to tail along the chain direction. This is one possible ground state for the arrangement of MNs dominated by magnetic dipolar interactions. The curved chain is likely the result of magnetic dipolar interaction influenced by a collective Brownian movement in solution and/or additional shear forces during the

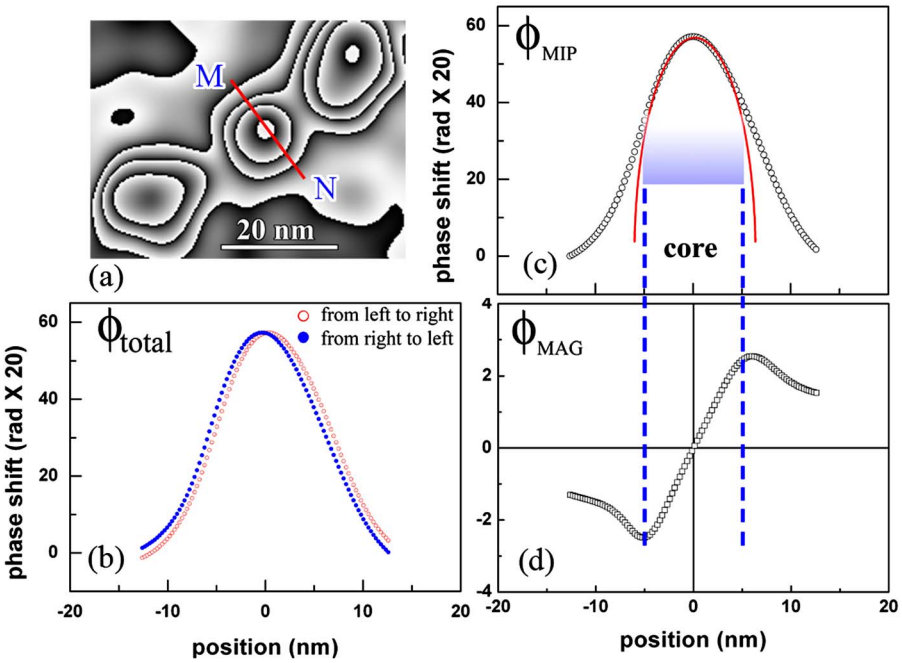

FIG. 3. (Color online) (a) Reconstructed phase image of the nanocrystal arrowed in Fig. 2. Profiles of the total phase shift ϕ_{total} (b), the contribution of the mean inner potential ϕ_{MIP} (c), and the contribution of the magnetic induction (d) ϕ_{mag} are plotted against position along *MN* cross the nanocrystal, as shown in (a). ϕ_{total} is recorded at two remanence states which are saturated along the left-to-right and right-to-left directions, respectively. It is found that the diameter of the cobalt core and the thickness of the CoO shell are 11.2 and 4.9 nm. The mean inner potential of Co core is estimated at 18.7 V, while that of CoO shell is about 16.1 V. The red solid curve in ϕ_{MIP} is the theoretical fit curve.

drying process. The shape and the density of the magnetic contours remained stable even when the specimen was heated *in situ* up to 200 °C. This observation indicates that the effective anisotropy energy KV of Co/CoO particles is much higher than the energy of thermal activation k_BT. An increase in the effective anisotropy energy from the exchange coupling between the core and shell in such $FM_{core}AFM_{shell}$ has been also reported in Ref. 6. According to Eq. (1), ϕ_{MIP} and ϕ_{mag} can be obtained by half of the sum and half of the difference of the phase images observed with the nanocrystal magnetized in opposite directions. The phase shifts of ϕ_{total}, ϕ_{MIP}, and ϕ_{mag} are plotted against the position along MN in Fig. 3(a) [see Figs. 3(b)–3(d)]. It is found that the magnetic contribution of the core lead to an asymmetry in the profile of the total phase shift ϕ_{total}. It is estimated from Figs. 3(c) and 3(d) that maximum phase shifts induced by the mean potential and the magnetic induction are 2.67 and 0.25 rad, and the diameter of the cobalt core and the thickness of the CoO shell are about 11.2 and 4.9 nm, respectively. It is also evaluated that the mean inner potential of Co core is about 18.7 V with an assumption of B_s^{Co} =1.7 Tesla, while that of CoO shell is about 16.1 V. The tails appearing on both sides of ϕ_{MIP} curve come from the surfactants on the particle surfaces. A decrease in the modulus of ϕ_{mag} measured out of the core, as shown in Fig. 3(d), results from a magnetic flux leakage.

The geometry of core-shell Co/CoO nanocrystal and the spin arrangement have been investigated by electron holography. It has been found that the CsMN consists of a 11 nm diameter ε-Co core and a 5-nm-thick CoO shell. The mean inner potentials of Co core and CoO shell have been evaluated at 18.7 and 16.1 V, respectively. It has also been found that the thermal stability of the 11.2 nm Co FM core is improved by the CoO AFM shell due to the exchange coupling between them.

One of the authors (Y.G.) gratefully acknowledges support from the 21st century COE program of Materials Research Center, Tohoku University. Work at the University of Washington was supported by NSF/DMR under Grant Nos. 0203069 and 0501421 and by the Campbell Endowment. Another author (Y.B.) acknowledges partial support from UW/PNNL Joint Institute of Nanoscience.

[1] F. Caruso, Adv. Mater. (Weinheim, Ger.) **13**, 11 (2001).
[2] E. Matijevic, in *Fine Particle Science and Technology*, edited by E. Pelizetti (Kluwer, Dordrecht, The Netherlands, 1996), pp. 1–16.
[3] L. M. Liz-Marzan, M. Giersig, and P. Mulvaney, Langmuir **12**, 4329 (1996).
[4] R. Partch, in *Materials Synthesis and Characterization*, edited by D. Perry (Plenum, New York, 1997), pp. 1–17.
[5] E. E. Carpenter, S. Calvin, R. M. Stroud, and V. G. Harris, Chem. Mater. **15**, 3245 (2003).
[6] H. Zeng, J. Li, J. P. Liu, Z. L. Wang, and S. Sun, Nature (London) **420**, 395 (2002).
[7] V. Skumryev, S. Stoyanov, Y. Zhang, G. Hadjipanayis, D. Givord, and J. Nogues, Nature (London) **423**, 850 (2003).
[8] C. C. Berry and A. S. G. Curtis, J. Phys. D **36**, R198 (2003).
[9] Y. Bao and Kannan M. Krishnan, J. Magn. Magn. Mater. **293**, 15 (2005).
[10] D. A. Thompson and J. S. Best, IBM J. Res. Dev. **44**, 311 (2000).
[11] Y. Bao, A. B. Pakhomov, and K. M. Krishnan, J. Appl. Phys. **97**, 10J317 (2005).
[12] Y. Bao, M. Beerman, A. B. Pakhomov, and K. M. Krishnan, J. Phys. Chem. B **109**, 7220 (2005).
[13] Y. Bao, M. Beerman, and K. M. Krishnan, J. Magn. Magn. Mater. **266**, 245 (2003).
[14] Y. Gao, Y. Bao, A. B. Pakhomov, D. Shindo, and K. M. Krishnan, Phys. Rev. Lett. **96**, 137205 (2006).
[15] D. Dinega and M. G. Bawendi, Angew. Chem., Int. Ed. **38**, 1788 (1999).
[16] Y. Gao, Y. Bao, M. Beerman, A. Yasuhara, D. Shindo, and K. M. Krishnan, Appl. Phys. Lett. **84**, 3361 (2004).
[17] D. Shindo and T. Oikawa, *Analytical Electron Microscopy for Materials Science* (Springer, Tokyo, 2002), pp. 116–126.
[18] R. E. Dunin-Borkowski, M. R. McCartney, D. J. Smith, and S. S. P. Parkin, Ultramicroscopy **74**, 61 (1998).